

SYSTEM SIMULATION OF RESIDENTIAL SIMULTANEOUS SPACE CONDITIONING AND WATER HEATING USING CO₂

J. K. RAJAN^(a), C. W. BULLARD^(b)

^(a) GE Energy Turbine Technology, PO Box 648, Greenville, SC 29602 USA
+1-864-241-6371, john.rajan@ge.com

^(b) University of Illinois at Urbana-Champaign, 1206 W. Green Street, Urbana, IL 61801 USA
+1-217-333-1942 (fax), bullard@uiuc.edu

ABSTRACT

The high heat rejection temperature of the transcritical CO₂ cycle creates opportunities for meeting domestic water heating needs in addition to space heating and air conditioning. This paper presents a complete analysis of a residential CO₂ space conditioning and water heating system design, across a wide ambient temperature range. The system simulation analysis builds upon a previous design study where a thermodynamic cycle analysis identified an optimal configuration where the water heater is placed downstream of the compressor before the refrigerant enters the gas cooler. The indoor and outdoor coils are cross-counterflow finned tube heat exchanger designs, and the water heater and internal heat exchanger are three-layer microchannel sandwich designs that can be rolled up in a scroll to save space. The geometric dimensions for each heat exchanger were optimized at separate ambient design conditions.

1. INTRODUCTION

The use of CO₂ in refrigeration and heat pump systems been the focus of renewed research and testing since Lorentzen re-introduced the idea of the transcritical cycle (Lorentzen, 1994). Since then, many papers have been published explaining the characteristics of prototype CO₂ systems. Neska *et al* (1998) designed and tested a CO₂ water heater prototype, and experimental results from other prototype space conditioning systems for cars and buildings are now available. This paper presents the design and analysis of a complete system simulation analysis of a combined residential space conditioning and water heating system. The system heats water to the typical U.S. storage temperature of 60°C, in addition to meeting space heating and cooling loads.

The optimal operating strategy for such a system varies throughout the year because the transcritical CO₂ cycle exhibits a COP-maximizing discharge pressure, with a discharge temperature that may lie above or below the desired hot water temperature. The system simulation results: verify the optimal operating strategies predicted by the previous thermodynamic cycle analysis (Rajan and Bullard, 2004); provide insight into choice of design conditions for each component; and reveal limitations in the ability of the actual system to meet ideal efficiency. The following section details the design assumptions for each heat exchanger. Then, the results of the system simulation models will be compared with the simple thermodynamic cycle predictions.

2. HEAT EXCHANGER DESIGN

The system simulations were made using Engineering Equation Solver (EES, Klein and Alvarado, 2005). The system schematic is shown in Figure 1. It is designed for the U.S. market with a 10.5 kW cooling capacity at the standard ARI-A condition where $T_{amb} = 35^{\circ}\text{C}$ (95°F). Space heating and cooling loads are approximated as linearly dependent on ambient temperature and based on an overall UA value from a moderately insulated house (Richter *et al*, 2001), with natural ventilation assumed between 15-20°C. The indoor and outdoor coils are of the cross-counterflow finned-tube type. The CO₂-to-water heat exchanger and internal heat exchanger are a simple sandwiches of three

microchannel tubes, and can be rolled into a scroll in order to save space. Each heat exchanger was designed at an appropriate ambient temperature condition with a specified set of criteria. To optimize the geometries for each heat exchanger, the detailed finite-volume submodel for that particular component was inserted into the simpler cycle model, where the rest of the components were simulated by simple thermodynamic equations.

The outdoor and indoor coils were sized for the for the $T_{amb} = 35^{\circ}\text{C}$ summer design condition. Both have 3 rows of 7 mm tubes and plain fins at 1.5 mm pitch. The outdoor coil was sized to meet a relatively stringent packaging constraint of $\sim 1.1 \text{ m}^2$ face area and its volumetric air flow rate was kept constant at $0.83 \text{ m}^3/\text{s}$ to limit fan noise. The outdoor coil performance

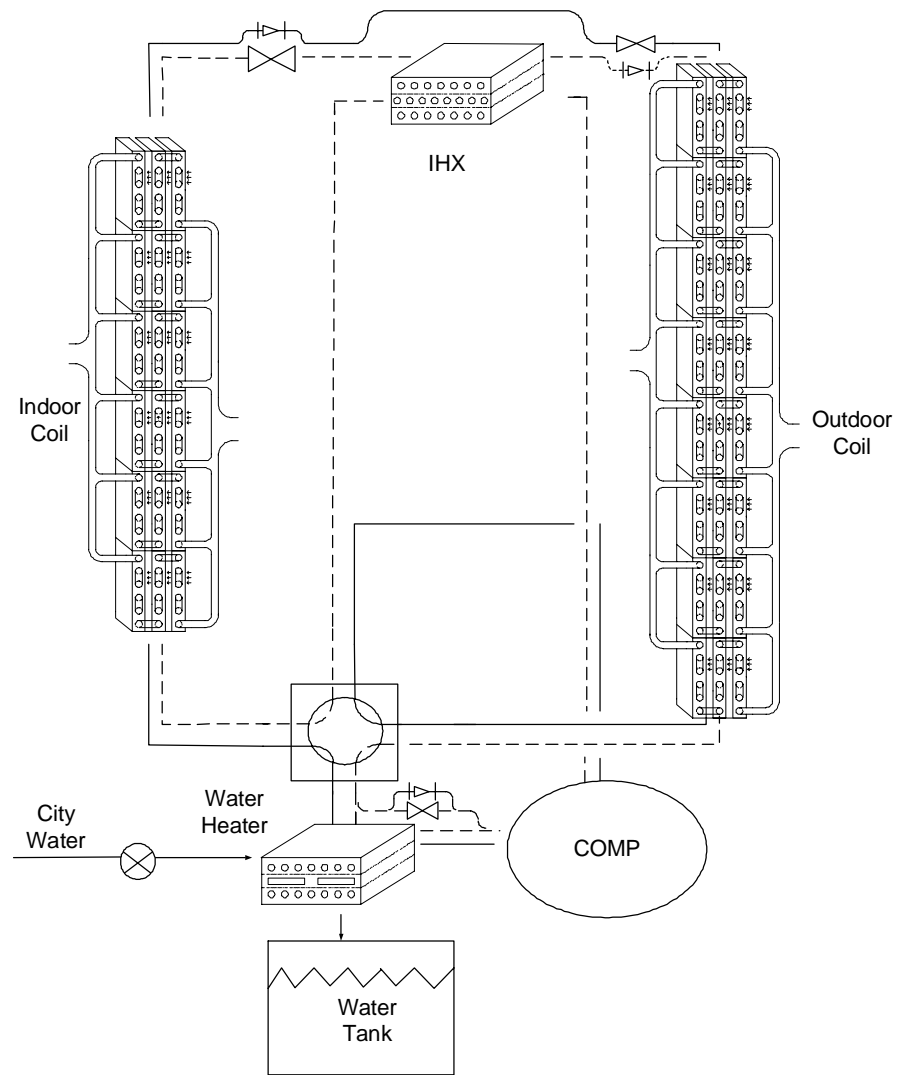


Figure 1. Space conditioning and water heating system

targets called for 2°C approach temperature differences at nearly all conditions and a maximum high side refrigerant pressure drop of 100 kPa. The indoor coil was sized for 10.5 kW cooling capacity at $26.7/19.4^{\circ}\text{C}$ (db/wb) with a sensible heat ratio (SHR) = 0.75 for dehumidification, and a saturation temperature drop of 0.5°C at the a/c design condition. Its face velocity was set to 1 m/s at the 35°C ambient design condition, but varied as necessary to satisfy the dehumidification requirement in summer, and to heat room air from 20°C return to 40°C supply in winter.

The microchannel water heater was sized for 3-hour recharge at $T_{amb} = 23.5^{\circ}\text{C}$ where the simple cycle calculations predicted the largest UA requirement (smallest difference between the CO_2 discharge gas and city water inlet temperature; see Figure 2). Since the CO_2 pressure drop through the water heater could become excessive at $T_{amb} = 40^{\circ}\text{C}$, the water heater pressure drop was limited to 40 kPa at $T_{amb} = 23.5^{\circ}\text{C}$ where the refrigerant mass flow rate was greatest. Typical tap water supply pressures are about 275 kPa to enable use in multistory buildings, so the maximum water side pressure drop was arbitrarily limited to 20% of that amount.

Simple cycle calculations had demonstrated that the IHX increases system efficiency only during the a/c season, at high ambient temperatures. It was therefore optimized for the $T_{amb} = 35^{\circ}\text{C}$ design condition. Like the indoor and outdoor coils, its detailed finite volume heat exchanger equations were inserted into the simple thermodynamic cycle model to determine the effects on system COP. As in the water heater, IHX performance was maximized by selecting the smallest available refrigerant port diameters of 0.5 mm and increasing the number of ports accordingly. This small compact IHX with 0.9 effectiveness significantly increased system COP; additional material costs would yield diminishing returns.

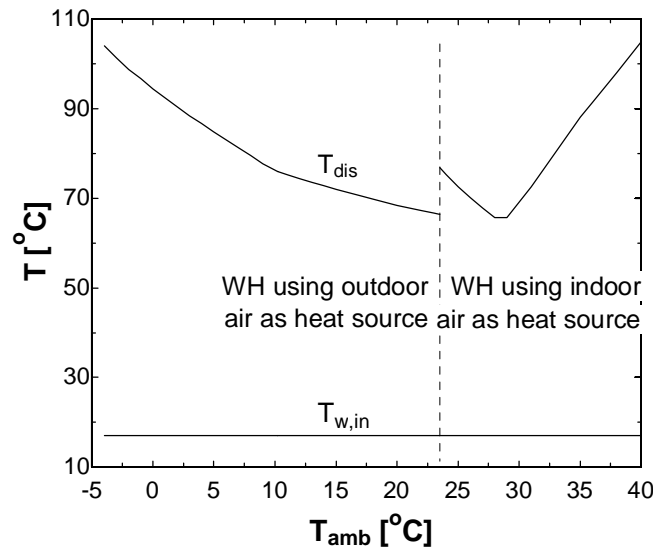


Figure 2. ΔT is smallest at $T_{amb} = 23.5^{\circ}\text{C}$

3. COMPARING SYSTEM SIMULATIONS WITH SIMPLE THERMODYNAMIC CYCLE ANALYSIS

This section compares system performance from the simple thermodynamic and detailed system simulations at several key ambient temperatures to show how well the real system matches the ideal predicted efficiency and energy use. The system model falls short of idealized efficiencies due to the nonzero CO_2 pressure drop, especially in the outdoor coil.

3.1 Simultaneous a/c and water heating

First consider the 35°C ambient condition at which the indoor and outdoor coil designs should be sized. Figure 3 shows a/c P-h diagrams at $T_{amb} = 35^{\circ}\text{C}$ for four cases: 1) the ideal cycle at its optimal discharge pressure; 2) outdoor coil simulated with the rest of components represented by ideal cycle equations without re-optimizing discharge pressure; 3) the same model at optimal discharge pressure; and 4) the complete system model.

Table 1. Optimizing a/c performance at $T_{amb} = 35^{\circ}\text{C}$

Case	$\text{COP}_{\text{cycle}}$	ΔP_{oc} (kPa)	Q_{oc} (kW)	m_r (kg/s)	$\Delta T_{\text{app,oc}}$ ($^{\circ}\text{C}$)
1. Simple cycle, Optimum	4.02	0	13.1	0.072	2
2. OC in Simple cycle	3.41	85	13.6	0.084	3.6
3. OC in Simple cycle, Optimum	3.84	44	13.2	0.067	1.7
4. System model, Optimum	3.59	31	13.4	0.066	1.7

Table 1 shows pressure drop, $\text{COP}_{\text{cycle}}$ (without fans), CO_2 mass flow rate, and outdoor coil capacity for the cases shown in Figure 3. The diagrams for cases 3 and 4 are almost identical, suggesting that the other components have almost negligible effects on outdoor coil performance, and only a small effect on system efficiency. Figure 3 illustrates an interesting characteristic of the transcritical cycle. The real outdoor coil geometry was well within the pressure drop constraint when simulated in the simple thermodynamic cycle model. However even 85 kPa (at the thermodynamically optimal design refrigerant flow rate) was large enough to cause the CO_2 to exit the outdoor coil and enter the evaporator at a higher enthalpy, substantially reducing COP. Re-

optimizing the discharge pressure then regains most of the loss, moving the exit state above the knee in the isotherm to a lower enthalpy. So COP_{cycle} decreases by only 4% for case 3, then pressure drops in the IHX and evaporator cause an additional 4% decrease for case 4. Overall fan/motor efficiencies of 20% in the real system (neglected in the simple cycle analysis) account for the additional 2% COP loss as reflected in Case 4.

With the real system operating at a higher discharge pressure than determined in the simple cycle analysis, the water heater sized for the lower temperature difference cools the refrigerant below $T_{amb} = 35^\circ\text{C}$. At such conditions the outdoor fan can be turned off so the cool CO_2 passes through the outdoor coil with only a <30 kPa pressure drop penalty.

Figure 5 shows that the simultaneous a/c and WH cycle has the same optimum P_{dis} as the a/c only cycle at $T_{amb} = 35^\circ\text{C}$. However its cycle efficiency is greater ($COP_{cycle} = 5.1$ for WH & a/c, and 3.7 for a/c only) due to the colder heat sink (17°C city water).

At $T_{amb} = 35^\circ\text{C}$, rejecting heat to water for 1.6 hours thus reduces the total system operating cost. Pressure drops in the simultaneous water and space heating mode impose a 10% efficiency penalty as shown in Table 2. Figure 5 also shows that at $T_{amb} \leq 28^\circ\text{C}$, simultaneous a/c and WH requires a higher P_{dis} than a/c only, in order to maintain the desired water supply temperature. As a result, the water heating starts to add cost to a/c (0.22 kWh/day extra at $T_{amb} = 28^\circ\text{C}$, $COP_{wh} = 55.0$). Note that COP_{wh} is based on the incremental power required for water heating; it is infinite on warmer days when a/c heat rejection alone is sufficient to provide it. Table 2 compares ideal to real system performance.

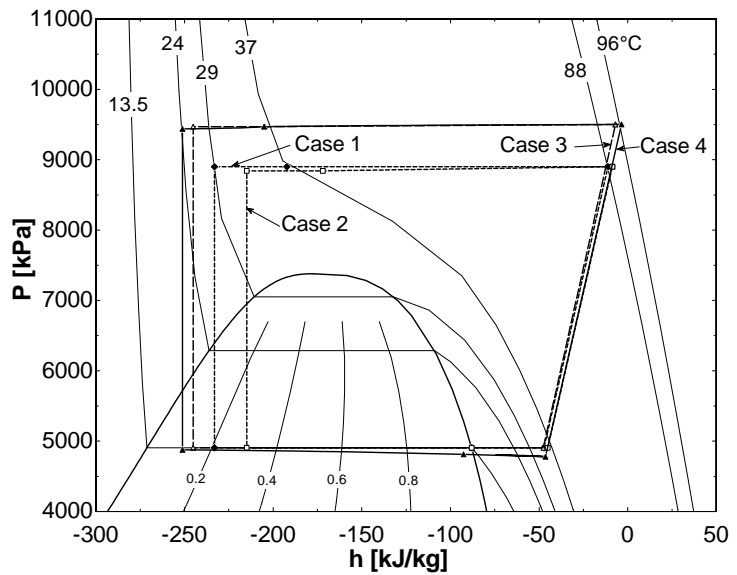


Figure 3. P-h diagrams at $T_{amb} = 35^\circ\text{C}$

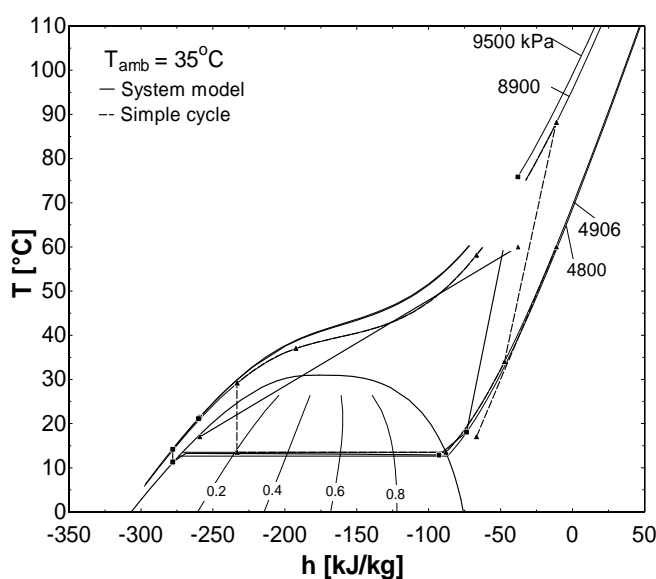


Figure 4. a/c and WH at $T_{amb} = 35^\circ\text{C}$

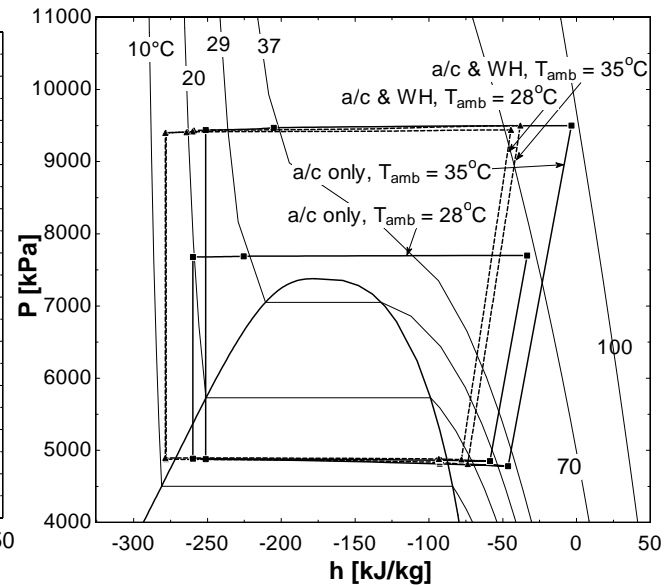


Figure 5. P-h diagrams at 35°C , 28°C

3.2 Tandem operation: space and water heating

Tandem operation minimizes energy use during the heating season because water heating load is accommodated in a separate heat pumping cycle apart from space heating. It is slightly more efficient than forcing the heat pump to simultaneously meet space and water heating loads. At $10 < T_{amb} < 15^{\circ}\text{C}$, both space and water heating loads can be met in less than 24 hours by cycling the compressor at its minimum speed of 30 Hz (at different optimal discharge pressures). At $-2 < T_{amb} < 10^{\circ}\text{C}$, the system must meet daily space heating loads in less than 24 hours, leaving time for the same system to meet water heating loads. As the simple thermodynamic analysis revealed, it is most efficient to use a backpressure valve to optimize the discharge pressure for water and space heating while the compressor is running, with no need to change its speed.

Table 2 shows the idealized simple cycle (sc) and real system (rs) models' predicted performance for space conditioning and water heating at several ambient temperatures. These results demonstrate clearly the severe penalty that would be associated with optimizing the entire system around the a/c design condition. Recall that the water heater had to be sized at 23.5°C where ΔT was minimum in order to operate near the optimal discharge pressure. At the coldest ambient temperatures the effect of outdoor coil pressure drop is greatest, because it is operating as an evaporator at low pressure where refrigerant volume is greater. Therefore the pressure drop constraint was applied at the -2°C and the coil was circuited accordingly. Despite the fact that the resulting 85 kPa pressure drop satisfied the constraint at the thermodynamically optimal discharge pressure for 35°C ambient operation, it caused a 4% COP loss at that condition. Therefore an outdoor coil with 4 slabs and more parallel circuits was simulated for comparison purposes. While it would have satisfied the stringent face area constraint, and nearly matched the simple cycle efficiency for both the heating and a/c design conditions, the extra slab would have increased the metal mass of the outdoor coil by 33%.

Table 2. Performance at different outdoor temperatures (fan/blower power omitted)

Characteristic	T_{amb} ($^{\circ}\text{C}$)			
	-1	15	28	35
$E_{tot,sc} / E_{tot,sm}$ (kWh/day)	72.4 / 84.7	8.3 / 8.8	21.1 / 22.7	62.7 / 67.4
$E_{wh,sm}$ (kWh/day) / $\text{COP}_{wh,sm}$	4.77 / 2.53	2.16 / 5.58	- 0.18 / ∞	- 0.75 / ∞
$t_{wh,sc}$, $t_{wh,sm}$ (hrs/day)	0.95 / 0.9	1.87 / 1.69	3 / 1.66	3 / 0.97
DT_{app} ($^{\circ}\text{C}$): OC / IC / WH	0.67 / 3.6 / 1.7	0.59 / 4.1 / 1.9	0.88 / 1.21 / 2.9	1.7 / 1.6 / 4.5
DP_r (kPa) OC / IC / WH	76 / 21 / 52	15 / 8.0 / 24	11 / 21 / 32	31 / 64 / 67
w_{comp} a/c or SH / WH	108 / 90	30 / 30	40 / 33	82 / 58
Q (kW) OC / IC / IHX / WH	11.8 / 8.4 / -- / 13.4	5.7 / 4.8 / -- / 7.2	7.1 / 6.2 / 1.2 / 7.3	13.4 / 10.5 / 3.1 / 12.5

* Note: Outdoor coil (OC), and indoor coil (IC) results are for space conditioning when water heating is off.

Table 2 compares compressor energy use and cycle efficiencies, neglecting fan and blower power to emphasize how the real cycle differs from the thermodynamically ideal one, even for modest departures from component design targets. It demonstrates that even small deviations from the target design criteria can. For example at the coldest condition the 76 kPa evaporator pressure drop corresponds to a saturation pressure drop of $\sim 1^{\circ}\text{C}$ rather than the target 0.5°C , and the 3.6°C approach temperature difference appears only slightly larger than the target 2°C , but causes a substantial shortfall in COP_{cyc} .

Table 2 also shows that the real system's water heating cycle adjusts to heat water slightly faster, due to the real system's slightly higher discharge temperature and pressure. The same higher-than-optimal high-side pressure and temperature increases the air-refrigerant temperature difference, which reduces approach temperature difference, albeit less efficiently than adding UA. The real system's nonzero pressure drop also affects the low end of the ambient range where tandem space

and water heating can meet 100% of the load ($T_{amb} = -2^{\circ}\text{C}$ for the real system vs. -4°C for the ideal cycle) where the compressor operates at its 120 Hz maximum. At outdoor ambient temperatures $<2^{\circ}\text{C}$ the system requires supplemental heating to meet space and water heating loads. Water heating is more than twice as efficient as electric resistance over the entire range of climate conditions.

Figure 6 shows how the P-h diagrams from the system model differ from the simple cycle to accommodate tandem water and space heating at $T_{amb} = -1^{\circ}\text{C}$. Here the relatively large approach temperature difference in the outdoor coil (acting as the evaporator) combines with the 76 kPa refrigerant pressure drop to increase the pressure lift and cause the SH cycle to optimize at a substantially higher discharge pressure (8200 kPa vs. 7500 kPa).

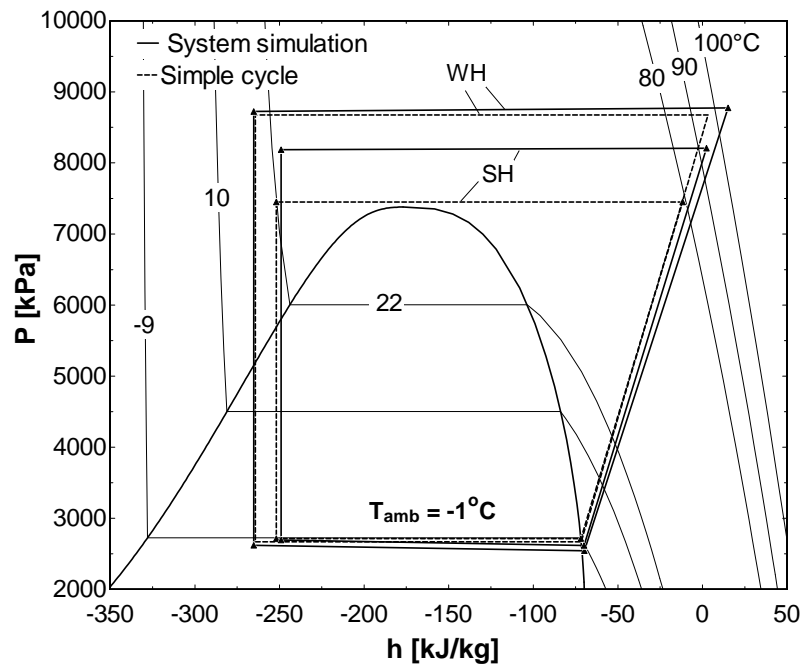


Figure 6. P-h diagram of Tandem space heating at $T_{amb} = -1^{\circ}\text{C}$

4. SUMMARY

These simulations of a real CO₂ system illustrate the importance of sizing and circuiting all the heat exchangers at different design conditions, in order to achieve near-ideal system performance across the entire range of operating conditions. For relatively mild climates where temperatures generally exceed 0°C , the outdoor coil and internal heat exchanger should be sized ($\Delta T_{approach} \approx 2^{\circ}\text{C}$) for the 35°C a/c rating condition, while the indoor coil should be sized for operating in gas cooler mode at the coldest outdoor temperature. The outdoor coil should be circuiting for operation in evaporator mode, to achieve a saturation temperature drop $\approx 1^{\circ}\text{C}$ at the coldest outdoor temperature. In the example shown here, the indoor coil was circuiting to meet the same saturation temperature drop constraint at the a/c design condition, and performed well in heating mode. The water heater needs to be sized for operation at the mildest outdoor temperatures where the gas cooler's driving temperature difference is smallest. Following these guidelines it should be possible to design components that will enable the system to operate very near ideal efficiency. Finally because system efficiency is so sensitive to gas cooler pressure drop when the thermodynamically optimal discharge pressure is very near the critical point, it may be cost-effective to bypass the water heater while operating in a/c-only mode. Since the ideal cycle analysis showed that internal heat exchanger provides little benefit in space heating mode, it should certainly be bypassed in order to avoid incurring severe pressure drop penalties which would be largest on the coldest winter days.

For systems that must operate in colder climates, the compressor and indoor and outdoor coils must be sized for the maximum heating load to minimize the need for supplemental electric resistance heat. The same guidelines for circuiting and for bypassing the water heater and internal heat exchanger apply.

Many of the assumptions used in this analysis need not apply to actual systems designed in the future. For example plain fins were assumed because the available correlations are based on very large sets of data, including low face velocities sometimes needed to achieve adequate

dehumidification, while the available slit and louver fin correlations have a more limited range. The assumption of 7 mm round tubes may also be superseded by flat tube heat exchanger technology, but future research on frost tolerant geometries may lead to configurations to which existing air-side correlations may not apply. Finally if microchannel heat exchangers are used, lower air- and refrigerant-side pressure drops will be easier to achieve, but much research needs to be done to achieve more uniform refrigerant distribution in both heat exchangers in evaporator mode.

NOMENCLATURE

<i>a/c</i>	air conditioning	(-)			<i>Subscripts</i>
<i>COP</i>	coefficient of performance	(-)		app	approach
<i>E</i>	energy per day	(kWh/d)		amb	ambient
<i>IC</i>	indoor coil	(-)		comp	compressor
<i>IHX</i>	internal heat exchanger	(-)		dis	discharge
<i>m</i>	mass flow rate	(kg/s)		evap	evaporator
<i>OC</i>	outdoor coil	(-)		oc	outdoor coil
<i>P</i>	pressure	(kPa)		r	refrigerant
<i>Q</i>	heat rate	(kW)		sat	saturated
<i>SH</i>	space heating	(-)		sc	space conditioning
<i>T</i>	temperature	(°C)		sh	space heating
τ	water heating time	(h/d)		sm	system model
<i>WH</i>	water heating	(-)		tot	total
				w, in	water inlet
				wh	water heater

REFERENCES

Klein, S.A., Alvarado, F.L, Engineering Equation Solver, v. 6.881-3D, F-Chart Software, Madison WI, 2003.

Lorentzen, G., 1994. Revival of carbon-dioxide as a refrigerant, *Int. J Refrig.*, vol 17, no 5: p. 292-301

Neksa, P., Håvard Rekstad, G. Reza Zakeri and Per Arne Schiefloe, 1998, CO₂-heat pump water heater: characteristics, system design and experimental results, *Int. J Refrig.*, vol 21, no 3: p. 172-179.

Rajan, J., Bullard, C., 2004. Residential space conditioning and water heating with transcritical CO₂ refrigeration cycle. 10th International Refrigeration and Air Conditioning Conference at Purdue, West Lafayette, IN, U.S.

Richter, M. R., C. W. Bullard, and P. S. Hrnjak, 2001, "Effect of Comfort Constraints on Cycle Efficiencies," Proc.International Mechanical Engineering Congress and Exposition, New York, NY.

ACKNOWLEDGEMENT

This project was supported by Samsung Electronics Co. Ltd.

